

Application of a novel optimization-based approach to characterize integrated signalling, regulatory, and metabolic biochemical networks

Jong Min Lee*, Erwin P. Gianchandani**
James A. Eddy**, Jason A. Papin**

*Department of Chemical and Materials Engineering, University of Alberta, Edmonton, AB T6G 2G6
CANADA (Tel: 780-492-8092; e-mail: jongmin.lee@ualberta.ca).

**Department of Biomedical Engineering, University of Virginia, Box 800759, Health System, Charlottesville, VA 22908 USA

Abstract: Extracellular cues affect signaling, metabolic, and regulatory processes to elicit cellular responses. Although intracellular signaling, metabolic, and regulatory networks are highly integrated, previous analyses have largely focused on independent processes (e.g., metabolism) without considering the interplay that exists among them. In this paper, we present the recent development of a flux balance analysis (FBA)-based strategy, referred to as integrated dynamic FBA (idFBA), that dynamically simulates cellular phenotypes arising from integrated networks [Lee et al., 2007]. The idFBA framework solves a linear program to find the optimal fluxes of biochemical reactions in an integrated network. It assumes quasi-steady-state conditions for “fast” reactions and incorporates “slow” reactions into the stoichiometric relationships to confine the feasible solution space. We also describe its recent application to a prototypic integrated system to assess the efficacy of idFBA [Lee et al., 2007].

1. INTRODUCTION

Intracellular biochemical networks are comprised of signaling, metabolic, and regulatory processes. Until recently, signaling, metabolic, and regulatory networks had largely been treated separately. However, high-throughput experimental data coupled with computational systems analysis techniques have elucidated multifunctional components involved in fundamental disease processes [Gianchandani et al., 2006]. For example, signaling cascades are triggered by the presence of extracellular stimuli and often result in activation of transcription factors. These transcription factors function in regulatory networks, regulating the transcription of associated genes and the synthesis of various proteins used in signal transduction and metabolism. Consequently, a key challenge in the post-genomic era is to consider the interconnectedness of biochemical networks and how extracellular cues affect highly integrated intracellular processes to elicit cellular responses such as growth or differentiation.

Two major approaches have been employed to quantitatively analyze large-scale biochemical networks: kinetic models [Famili et al., 2005] and flux balance analysis (FBA) [Kauffman et al., 2003]. In the first approach, a set of ordinary differential equations (ODEs) describing the mass balance of each species in the system is constructed. Despite its generality, the application of this type of mechanistic model at a genome-scale is largely considered impractical because it necessitates the consideration of many pathways for which detailed reactions and their kinetic parameters are not yet known. On the other hand, FBA can accurately generate phenotypic properties of a biological network in the form of a steady-state flux (i.e., reaction rate) distribution without detailed kinetic information. FBA only requires a physiologically relevant objective function (e.g., in the case

of metabolism, maximizing the growth rate or maximizing ATP production), mass-balance constraints (i.e., the stoichiometry of the reactions), and constraints on reaction directions and thermodynamics. Since the physicochemical constraints are readily defined (e.g., from the annotated genome sequence and measured enzymatic capacities), FBA has been used effectively to study large-scale biochemical networks, particularly metabolic networks [Papin et al., 2003].

A key challenge to the modeling of integrated systems is the multiple orders of magnitude that time scales of intracellular biochemical networks generally span. Signaling and metabolic reactions typically occur rapidly. For example, kinase/phosphatase reactions, protein conformational changes, and most metabolic reactions occur on the order of fractions of a second to seconds [Papin et al., 2005]. By contrast, receptor internalization [Lauffenburger and Linderman, 1993] and regulatory events [Weng et al., 1999], as well as end-stage phenotypic properties such as cellular growth or differentiation [Alberts, 2002] can take several minutes to hours to complete. These multiple time-scales pose computational challenges for the quantitative analysis of integrated systems. Kinetic models of integrated systems are inherently “stiff,” which are difficult to simulate and extremely sensitive to modeling errors [Kumar et al., 1998]. It is also challenging to apply FBA to integrated systems because of its intrinsic steady-state assumption, while the “fast” and “slow” reaction dynamics that coexist intracellularly. Due to these complexities, previous models and analyses have focused primarily on network modules rather than integrated systems. [Papin et al., 2004, Pritchard and Kell, 2002, Stelling and Gilles, 2001].

Some preliminary dynamic analyses of integrated systems have been completed. Integrated analyses of regulatory and metabolic networks revealed novel mechanisms in

Saccharomyces cerevisiae and *Escherichia coli* [Covert and Palsson, 2002, Herrgard et al., 2006]. Recently, a kinetic model accounting for signal transduction, metabolism, and regulation was constructed to describe the response of *S. cerevisiae* to osmotic shock [Klipp et al., 2005]. This model connected specific outputs of one network (e.g., signaling) with the inputs of another network (e.g., metabolism) in a “sequential” fashion. However, it did not consider the complete set of interactions among the biochemical networks, such as feedback of proteins expressed as a function of the regulatory network to signaling and metabolism.

The objective of this paper is to describe the recent development of a FBA-based computational framework, termed integrated dynamic flux balance analysis (idFBA), for the quantitative, dynamic analysis of cellular behaviors arising from signaling, metabolic, and regulatory networks at the genome-scale (see Lee et al. (2007)). The idFBA framework requires an integrated stoichiometric reconstruction of signaling, metabolic, and regulatory processes. It assumes quasi-steady-state conditions for “fast” reactions and incorporates “slow” reactions in a time-delayed manner. To assess the efficacy of idFBA, we describe its recent application to a prototypic integrated system with topological features characteristic of those observed in existing *in silico* signaling, metabolic, and regulatory network reconstructions as well as kinetic parameters reported in literature. idFBA allowed for quantitative, dynamic analysis of systemic effects of extracellular cues on phenotypes of the prototypic integrated system and provided acceptable time-course predictions when contrasted with an equivalent kinetic model.

2. CONCEPTUAL FRAMEWORK AND METHODS

2.1 Biological Systems Evaluated: Prototypic Integrated System

In order to assess the efficacy of idFBA, a prototypic integrated system was constructed with characteristics typical of those observed in published *in silico* network reconstructions of signaling, metabolic, and regulatory networks (Figure 1, see Lee et al. (2007)). Specifically, we generated representative reactions with stoichiometric relationships and estimated their associated rate constants from literature.

Signal transduction

Signal transduction pathways govern a cell’s response to extracellular stimuli. The prototypic signaling network is comprised of a set of reactions that is typical of biological signaling pathways such as phosphorelay and kinase cascade modules. As shown in Figure 1, ligands (L_1 , L_2 , and L_3) bind to receptors (R_1 , R_2 , and R_3) to form ligand-receptor complexes (L_1R_1 , L_2R_2 , and L_3R_3). These complexes are subsequently either internalized or involved in phosphorylation events. Phosphorylation of signaling components takes place through a series of reactions

involving ATP and other activated components. Any one signaling component can also activate multiple other signaling components. Ultimately, activated transcription factors (T1p, T2p, and T3p), that are representative of phosphorylated proteins are the downstream effector molecules that result from the signaling pathways.

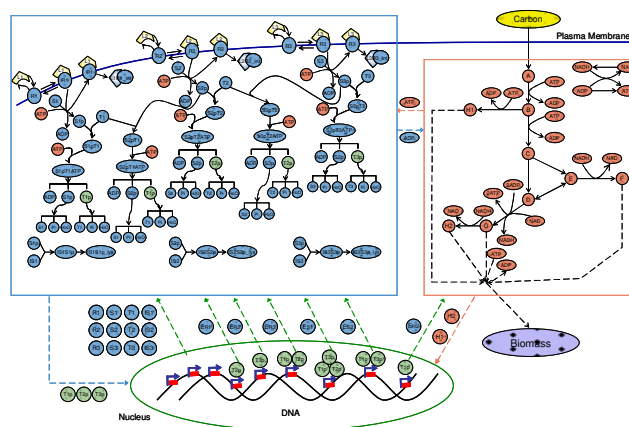
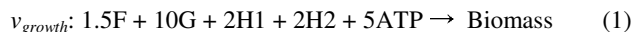


Figure 1. A prototypic integrated network. Solid boundary lines indicate three functional network modules: signal transduction (upper left), metabolism (upper right), and transcriptional regulation (bottom).

The model of signal transduction consists of a total of 45 reactions. The rate constants for these reactions are based on values observed for similar signaling reactions in literature [Klipp et al., 2005, Lauffenburger and Linderman, 1993, Schoeberl, et al., 2002]. Most of the reactions in the prototypic signaling network are “fast”; steady-state concentrations are achieved on the order of seconds. However, there are some “slow” reactions that take on the order of several minutes to hours to reach steady state. These include the internalization of ligand-receptor complexes and inhibition and hydrolysis of activated components. The typical order of magnitude of the concentrations of signaling components in this prototypic integrated system is micromolar (μM) [Klipp et al., 2005; Schoeberl, 2002].

Metabolism

Metabolic pathways produce energy, amino acids, and other precursors required for the growth and maintenance of a cell. The metabolic reactions in the prototypic system comprise pathways representative of glycolysis and amino acid synthesis. The model contains 13 reactions, and the associated kinetic parameters were adapted from previous work [Rizzi et al., 1997; Teusink et al., 2000; Klipp et al., 2005]. The biosynthetic requirements for cellular growth (i.e., biomass production) were defined based on the prototypic metabolic reactions in Covert et al. (2001) (Eq. (1)), where H1 and H2 are representative of amino acids and F and G are representative of metabolites.



The maximum carbon utilization rate, S_{umax} , was set to 10.5mmol/(g(dry weight)•h) as in Varma and Palsson, 1994. Most of the metabolic reactions in the model are “fast” and achieve steady states in several seconds. The growth of biomass is on the order of hours. The typical order of magnitude of metabolite concentrations is milli-molar (mM) [Teusink et al., 2000].

Regulation

Transcriptional regulatory networks control the transcription state of a genome. Inputs to regulatory networks are environmental cues, including the presence and absence of extracellular metabolites, reaction fluxes, and specific conditions such as pH values. The internal reactions, often not known in chemical detail, are represented by regulatory rules that describe the activation or inhibition of gene transcription in response to these environmental cues. The outputs are the synthesized protein products that result through a combination of the signaling inputs acting upon the regulatory rules as well as consequent transcription and translation. These networks have been mathematically described using a Boolean formalism, in which the state of a gene is represented as either transcribed or not transcribed in response to regulatory signals [Gianchandani, 2006].

The prototypic transcriptional regulatory network presented here is comprised of 18 genes. Three transcription factors are inputs to the system, and 18 protein products with functions in metabolism and signaling are outputs of the network. Of the 18 genes, six are regulated by the presence or absence of the transcription factors. The remaining genes are defined to be constitutively active. The transcriptional regulatory rules for the six regulated genes are described using a Boolean formalism. For example, the regulatory rule in (2) implies that Gene ER₃ is expressed only if both T_{1p} and T_{2p} are present.

$$\text{Gene ER}_3 = \text{IF} (T_{1p} \text{ AND } T_{2p}) \quad (2)$$

For simplicity, the amino acid requirements for protein synthesis are only considered for the proteins indicated in Figure 1.

2.2 Flux Balance Analysis (FBA)

FBA does require a stoichiometric reconstruction of the biochemical network of interest. This biochemical network reconstruction can be represented in matrix form, \mathbf{S} , where \mathbf{S} is of size m components \times n reactions and is comprised of stoichiometric coefficients that capture the mass ratios among the biochemical components of underlying reactions. After the network is reconstructed, fluxes are calculated at steady state by

$$\frac{d\mathbf{C}}{dt} = \mathbf{S} \cdot \mathbf{v} = \mathbf{0} \quad (3)$$

where \mathbf{C} is a m -row vector defining the concentrations of the m components within the system, and \mathbf{v} corresponds to the flux in the associated reaction (column).

Eq. (3) by itself generally leads to an under-determined system because the number of components tends to be far fewer than the number of reactions. Even with additional constraints, FBA usually requires performing an optimization with linear programming (LP) to identify the most likely flux distribution given a cellular objective. The objective is defined as

$$Z = \mathbf{c}^T \cdot \mathbf{v} \quad (4)$$

Common choices for cellular objective functions in models of metabolic networks include biomass production, energy, and byproduct production. Then, FBA attempts to solve the LP problem in (5) to find a physiologically relevant cellular phenotype in the form of a flux distribution \mathbf{v} that optimizes Z while lying in the bounded solution space defined by a set of physio-chemical, topological, and environmental constraints.

$$\begin{aligned} & \max_{\mathbf{v}} \mathbf{c}^T \cdot \mathbf{v} \\ & \text{subject to:} \quad \frac{d\mathbf{C}}{dt} = \mathbf{S} \cdot \mathbf{v} = \mathbf{0} \\ & \quad \quad \quad \mathbf{v}_{lb} \leq \mathbf{v} \leq \mathbf{v}_{ub} \end{aligned} \quad (5)$$

where \mathbf{v}_{lb} and \mathbf{v}_{ub} are the lower and upper bounds on the reaction fluxes, respectively. For instance, these constrain reaction directions. Though the steady-state assumption of FBA precludes dynamic concentrations of the network components, dynamic profiles of cellular phenotypes (e.g., cellular growth or differentiation) have been successfully predicted with a quasi-steady-state assumption [Varma and Palsson, 1994, Covert et al., 2001]. This assumption involves discretizing the time domain into intervals; and (1) solving the LP problem contained within FBA at the beginning of each interval, and (2) based on the resultant flux data, solving a system of ODEs for concentrations over time within each interval.

Applications of FBA to dynamic simulations have focused on metabolic networks because time constants of metabolic transients are typically very rapid. Exceptions include the incorporation of gene regulatory events, which are much slower than metabolic reactions, into FBA for time-course simulation of metabolic reactions [Covert et al., 2000, Covert et al., 2001]. In these cases, the regulatory constraints were described as Boolean operators and imposed in a time-delayed manner. However, these examples are limited to metabolic and regulatory processes and do not consider changes in the mass balance (e.g., protein synthesis) arising from the interactions between metabolic and regulatory processes and signaling systems.

2.3 idFBA: A FBA-based approach for the dynamic simulation of integrated systems

Applying FBA directly to integrated networks is challenging because objectives of signaling systems are not well-defined and integrated networks are comprised of reactions with mixed time scales. Here we describe the idFBA framework, including how we address these challenges using the prototypic integrated system.

FBA-based representation of signaling networks

As previously described, we represent signaling networks using a stoichiometric formalism. Transcription factors activate transcriptional regulatory programs in response to extracellular cues. Consequently, an obvious choice for the objective of a signaling network is maximizing the production of transcription factors. However, this objective by itself fails to generalize to a feasible flux distribution. Instead, maximizing the production of the transcription factor T_{1p} consistently yields zero fluxes for the key pathway reactions including receptor internalization, pathway inhibition, and transcription factor degradation.

To address this challenge, we model the objective of a signaling network by introducing a binary variable, $I(R_i)$, indicating the inclusion of a reaction R_i that has zero flux given a particular objective. The value of this binary variable is determined by a set of rules and parameters a user specifies, such as the time required for protein synthesis and degradation. It is multiplied by the upper bound of the associated reaction flux. If a particular reaction is included in the network based on the user-defined rules and parameters (i.e., it has a non-zero flux), the binary variables for the reactions sharing components with the included reaction are set to zero. For example, including the receptor internalization reaction ($L_1R_1 \rightarrow L_1R_{1,int}$) implies that the binary variables for the reactions ($L_1R_1 + S_1 \rightarrow L_1R_1 \cdot S_1$) and ($L_1R_1 \rightarrow L_1 + R_1$) are set to zero. In this manner, a feasible flux distribution for a signaling network is obtained by maximizing for the production of transcription factors.

Incorporation of slow reactions into FBA

In addition, to characterize mixed time-scale phenomena using FBA, we implement idFBA by assuming quasi-steady-state conditions for “fast” reactions and incorporating “slow” reactions into the stoichiometric matrix in a time-delayed manner as in Covert et al. (2001). In other words, we approximate continuous phenomena occurring over long time as instantaneous events at particular time points. Two parameters are used to implement this approach: time-delay (τ_{delay}), indicating after what time a “slow” reaction is considered an “active” steady-state constraint in the stoichiometric matrix; and reaction duration ($\tau_{duration}$), indicating how long the “slow” reaction remains as the effective constraint once it is activated. In the prototypic integrated system, “slow” reactions include protein degradation, pathway inhibition, and receptor internalization in the signaling network; the uptake of a carbon source and production of biomass in the metabolic network; and the synthesis of proteins in the transcriptional regulatory network.

Dynamic simulation of integrated systems

The optimized flux distribution that results from FBA is used to predict the time-course of phenotypic variables. The time-scale separation between “slow” and “fast” reactions is determined by the discretization of the time domain. Specifically, a reaction that reaches steady state or that produces a product at a specified threshold concentration within a single time step is considered “fast.” “Slow” reactions are those that take longer than the unit time interval to attain steady state.

Ultimately, the implementation of the idFBA framework can be discretized as a seven-step process (see Lee et al. (2007)). We summarize it below.

1. Discretize the time window into small steps, Δt .
2. Initialize a $R_s \times t_N$ incidence matrix (\mathbf{I}) denoting which reactions participate during which time steps. Here R_s represents the number of reactions within the system and t_N the number of time intervals.

$$\mathbf{I} = \begin{bmatrix} 0 & \cdots & 0 \\ \vdots & \ddots & \vdots \\ 0 & \cdots & 0 \end{bmatrix} \quad (6)$$

Each row of \mathbf{I} denotes a reaction R_i , and each column Δt . The coefficients of \mathbf{I} are binary variables indicating whether a given reaction participates during a given time step. A “0” denotes that a given reaction does not participate in the system, whereas a “1” denotes that the reaction does participate in.

3. For each reaction in the system R_i , multiply the corresponding coefficient, $\mathbf{I}(R_i, t)$, by the flux bounds of the reaction. The flux bounds of excluded reactions, if any, are multiplied by $[1 - \mathbf{I}(R_i, t)]$. By specifying $\mathbf{I}(R_i, t) = 1$ for the associated excluded reactions, the fluxes of these reactions are set to zero when a “slow” reaction is included.
4. Solve (5) for the optimized flux, \mathbf{v}^* , with the updated constraints, for the start of the current time step, $t_{current}$.
5. Given the optimized flux vector for $t_{current}$, integrate the phenotype variable, X_p , over the time step, Δt . Here we consider two phenotype variables, namely cell density (X) and substrate concentration (S_c). These terms are given by (8), where μ is a specific growth rate, and S_u is the uptake rate for the carbon source.

$$\frac{dX}{dt} = \mu \cdot X, \quad \frac{dS_c}{dt} = -S_u \cdot X \quad (8)$$

6. Update \mathbf{I} based on \mathbf{v}^* at the current time step given the time-delay and reaction duration parameters
- $$\mathbf{I}(R_i, t) = \begin{cases} 0, & t < t_{current} + \tau_{delay} \\ 1, & t_{current} + \tau_{delay} \leq t \leq t_{current} + \tau_{delay} + \tau_{duration} \end{cases} \quad (9)$$

7. Repeat steps 4 through 6. The optimized flux vector \mathbf{v}^* , at the current time step $t_{current}$ imposes new constraints on the internal fluxes of the next time step. These constraints include ligand binding rates, carbon uptake rate, and protein production rates.

3. RESULTS AND DISCUSSION

Using the prototypic integrated system shown in Figure 1, predictions of the dynamic characteristics of phenotypic variables (i.e., cellular growth and substrate consumption) were made for different conditions (see Lee et al. (2007)). We briefly describe how we demonstrated the effects of ligand availability and changes in regulatory rules on phenotype behavior.

3.1 Implementation Details

- The sample time, Δt , was set to 0.1h as in Varma and Palsson, 1994.
- The maximum carbon uptake rate, S_u^{max} , was set to $0.003 \frac{mmol}{gDCW \cdot s}$ as in Varma and Palsson, 1994.
- Constraints on the uptake of substrates and ligand binding rates were assumed to be available.
- The binary variable $\mathbf{I}(R_i, t)$ corresponding to the synthesis of a particular protein was set to 1 if the flux of the activated transcription factor exceeded a specified threshold ($0.01 \mu M/s$ as in Covert et al. (2001)). If the flux of a phosphorylated component was not zero, elements of \mathbf{I} for inhibition and degradation of the component were set to 1 after specified time delays and with durations of one sample time. This particular $\tau_{duration}$ was chosen since the steady-state constraints of these reactions impose complete depletion of available reactants within the current sample time. Similarly, elements of \mathbf{I} for the internalization of ligand-receptor complexes were set to 1 after a time delay accounting for the time it takes for the complexes to become internalized.
- The objective function of the resultant FBA formulations included maximizing the production of: (1) activated transcription factors in the signaling network; (2) the set of metabolites that produce biomass in the metabolic network; and (3) the amino acids, in relative ratios, that are necessary for the synthesis of proteins by the transcriptional regulatory network.

3.2 Evaluating effects of environmental cues

We first simulated the case in which the concentration of all three ligands was $2.0 \mu M$. The results are shown in Figure 2 (see Lee et al. 2007). The carbon source was completely depleted by $t = 8.7h$ from an initial concentration (or “dose”) of $10.5mM$. The production of the amino acid H2 was catalyzed by the enzyme with an initial delay of $\tau_{delay} = 40min$, and consequently, cellular growth was sluggish during this initial period. Two periods of no growth (i.e., at approximately $t = 7h$ and $t = 8.25h$) corresponded to times

when enzymes that catalyze metabolic reactions and protein synthesis were unavailable. For example, the first phase of no growth at $t = 7h$ was due to the degradation (and therefore inactivity) of transcription factors regulating key factors involved in biomass production, and the second at $t = 8.25h$ was caused by the degradation of phosphorylated proteins (e.g., S_{1p}) that activate transcription factors leading to protein synthesis. Although these types of on/off descriptions are not precise, they serve as useful approximations of the phenotypic behavior over an entire time course.

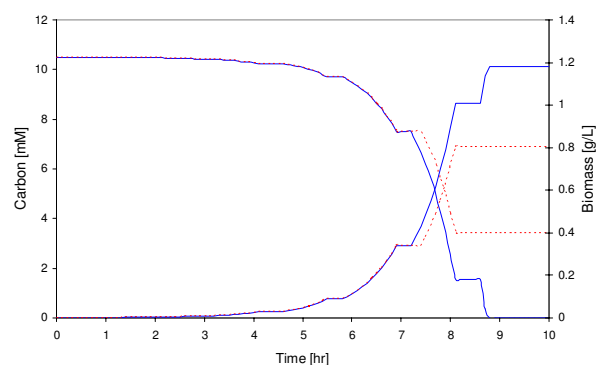


Figure 2. The solid lines represent the case where the concentrations of all the ligands are kept at $2.0[\mu M]$ during the entire simulation time. The dotted lines represent the case where no ligand is present during the time, $6.0 \leq t \leq 6.5$.

We subsequently simulated the case in which the ligands were temporarily unavailable for cellular uptake during the evaluated time-course (Figure 2). Specifically, no ligand was available for cellular uptake at $6.0h \leq t \leq 6.5h$. Consequently, a no-growth period was observed at about 7h. All transcription factors generated before $t=6h$ were degraded by this time, preventing the amino acid H2 from being synthesized for a period of 0.5h (i.e., until the ligand supply was restored). The cell also stopped growing at about $t = 8.2h$. The transcription factor T_{3p} , which activates the synthesis of enzyme in the integrated prototypic system, was not produced, leading to a lack of synthesis of the protein S_1 .

3.3 Comparison to a Kinetic-Based Model

The idFBA framework, as applied to the prototypic integrated system, was compared to a kinetic model that represented the reactions as ordinary differential equations [Lee et al., 2007]. These two approaches are completely independent: the idFBA framework requires only stoichiometric constraints and approximates the dynamics of the system with time-delay information, whereas the kinetic model requires all of the kinetic detail and yields a more accurate portrait of the system dynamics. For both implementations, we assumed an initial ligand concentration, $2.0 \mu M$, for all three ligands. We note that the following dynamic parameters for slow reactions were identified from the kinetic model and implemented as τ_{delay} and $\tau_{duration}$ in idFBA: the degradation of transcription factors, 5h, the delay in protein synthesis, 40min, the degradation of proteins, 4h, internalization, 5h, and inhibition, 5h. One striking result is

shown in Figure 3 (see Lee et al. (2007)). The growth times calculated by both approaches are comparable (computed as 4.9h for idFBA and 5.1h for the kinetic model), with a difference of just two time steps over a 51-time-step simulation. The discrepancy in the amount of biomass synthesized is a consequence of the kinetic-based model itself. Unlike in idFBA, all of the reactions in the metabolic network of the kinetic model are constitutively active. As a result, resources such as amino acids are used in other pathways, e.g., for the synthesis of surplus proteins, and as a result the amount of biomass produced is less than the value estimated by idFBA which simply maximizes for biomass production. Nevertheless, idFBA effectively approximates the dynamics of a system using purely the underlying network stoichiometry, efficaciously offering novel hypotheses that can serve as the basis for further experimental and computational study.

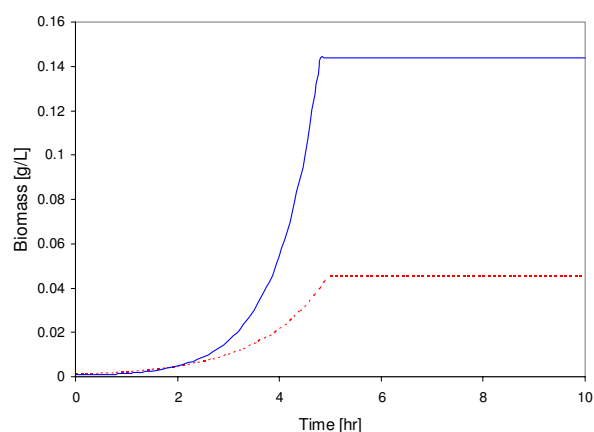


Figure 3. The dynamics of biomass production from idFBA (solid) and detailed kinetic-based (dotted) approaches.

ACKNOWLEDGEMENTS

We thank Markus W. Covert for helpful discussions about implementing FBA. We also thank the National Institutes of Health (NIH) (GM08715/NIH Biotechnology Training Grant) for funding EPG.

REFERENCES

Alberts, B. (2002). *Molecular Biology of the Cell*, Garland Science, New York.

Covert, M.W. and B.O. Palsson (2002). Transcriptional regulation in constraints-based metabolic models of *Escherichia coli*. *J Biol Chem*, **277**, 28058-28064.

Covert, M.W., C.H. Schilling, and B.O. Palsson (2001). Regulation of gene expression in flux balance models of metabolism. *J Theor Biol*, **213**, 73-88.

Famili, I., R. Mahadevan, and B.O. Palsson (2005). k-Cone analysis: determining all candidate values for kinetic parameters on a network scale. *Biophys J*, **88**, 1616-1625.

Gianchandani, E.P., J.A. Papin, N.D. Price, A.R. Joyce, and B.O. Palsson (2006). Matrix formalism to describe functional states of transcriptional regulatory systems. *PLoS Comput Biol*, **2**, e101.

Herrgard, M.J., B.S. Lee, V. Portnoy, and B.O. Palsson (2006). Integrated analysis of regulatory and metabolic networks reveals novel regulatory mechanisms in *Saccharomyces cerevisiae*. *Genome Res*, **16**, 627-635.

Kauffman, K.J., P. Prakash, and J.S. Edwards (2003). Advances in flux balance analysis. *Curr Opin Biotechnol*, **14**, 491-496.

Klipp, E., B. Nordlander, R. Kruger, P. Gennemark, and S. Hohmann (2005). Integrative model of the response of yeast to osmotic shock. *Nat Biotechnol*, **23**, 975-982.

Kumar, A., P. Christofides, and P. Daoutidis (1998). Singular perturbation modelling of nonlinear processes with nonexplicit time-scale multiplicity. *Chemical Engineering Science*, **53**, 1491-1504.

Lauffenburger, D.A. and J.J. Linderman (1993). *Receptors: Models for Binding, Trafficking, and Signaling*, Oxford University Press, New York.

Lee, J.M., E.P. Gianchandani, J. Eddy, and J.A. Papin (2007). Characterizing signaling, metabolic, and regulatory networks with integrated dynamic flux balance analysis (idFBA). *PLoS Comp Biol*, in review.

Papin, J.A., T. Hunter, B.O. Palsson, S. Subramanian (2005). Reconstruction of cellular signalling networks and analysis of their properties. *Nat Rev Mol Cell Biol*, **6**, 99-111.

Papin, J.A. and B.O. Palsson (2004). The JAK-STAT signaling network in the human B-cell: an extreme signaling pathway analysis. *Biophys J*, **87**, 37-46.

Papin, J.A., N.D. Price, S.J. Wiback, D.A. Fell, and B.O. Palsson (2003). Metabolic pathways in the post-genome era. *Trends Biochem Sci*, **28**, 250-258.

Pritchard L. and D.B. Kell (2002). Schemes of flux control in a model of *Saccharomyces cerevisiae* glycolysis. *Eur J Biochem*, **269**, 3894-3904.

Rizzi, M, M. Baltes, U. Theobald, and M. Reuss (1997). In vivo analysis of metabolic dynamics in *Saccharomyces cerevisiae*. 2. Mathematical model. *Biotechnology and Bioengineering*, **55**, 592-608.

Schoeberl, B., C. Eichler-Jonsson, E.D. Gilles, and G. Muller (2002). Computational modelling of the dynamics of the MAP kinase cascade activated by surface and internalized EGF receptors. *Nat Biotechnol*, **20**, 370-375.

Stelling, J. and E.D. Gilles (2001). Robustness vs. identifiability of regulatory modules? the case of mitotic control in budding yeast cell cycle regulation. In: *Proceedings of the Second International Conference on Systems Biology*, 181-190.

Teusink, B., J. Passarge, C.A. Reijenga, E. Esgalhado, C.C. van der Weijden, et al. (2000). Can yeast glycolysis be understood in terms of in vitro kinetics of the constituent enzymes? Testing biochemistry. *Eur J Biochem*, **267**, 5313-5329.

Varma, A. and B.O. Palsson (1994). Stoichiometric flux balance models quantitatively predict growth and metabolic by-product secretion in wild-type *Escherichia coli* W3110. *Appl Environ Microbiol*, **60**, 3724-3731.

Weng, G., U.S. Bhalla, R. Iyengar (1999). Complexity in biological signaling systems. *Science*, **284**, 92-96.